Ca^{2+}-Mobilization and Cell Contraction after Muscarinic Cholinergic Stimulation of the Chick Embryo Lens

Matthias Oppitz,[1] *Andreas Mack,*[2] *and Ulrich Drews*[1]

Purpose. In the embryonic lens, cells of the anterior epithelium proliferate, migrate through the equatorial zone, and elongate to form primary lens fibers at the posterior pole. During this stage of development, cholinesterase (ChE) activity has been described as in other embryonic tissues implicated in morphogenesis. The purpose of the study was to demonstrate in addition to ChE the presence of muscarinic acetylcholine receptors (mAChR) and choline acetyltransferase (ChAT) and to test whether the muscarinic cholinergic system is involved in the regulation of cellular movements.

Methods. In the chick embryo lens (Hamburger-Hamilton [HH] stage 21), the expression of mAChR and ChAT were demonstrated by immunohistochemistry. Isolated whole embryonic lenses were loaded with fura-2/AM, and changes of cytosolic calcium were measured after muscarinic stimulation. Size changes were assessed by morphometry with the use of time-lapse videos.

Results. mAChR was present in the equatorial zone of the lens and in the elongating primary lens fibers. Anti-ChAT immunoreactivity was restricted to the primary lens fibers. Addition of carbachol induced an intracellular Ca^{2+} peak followed by a plateau phase of extracellular Ca^{2+} influx. The plateau phase was reversed by addition of atropine. Concomitant with the calcium release, a contraction of the lens and an increase in opacity was observed.

Conclusions. The localization of ChAT in the differentiating fibers of the lens indicates that acetylcholine is synthesized during differentiation and modulates morphogenesis and elongation of mAChR-positive progenitor cells in the equatorial zone. The carbachol-induced contraction indicates that the embryonic muscarinic system may be involved in the regulation of cellular movements. (*Invest Ophthalmol Vis Sci.* 2003; 44:4813–4819) DOI:10.1167/iovs.03-0258

In the embryonic lens the phases of proliferation, cell migration, and differentiation are spatially separated. Proliferation occurs in the anterior lens epithelium, migration in the equatorial zone, and differentiation at the posterior pole of the lens. According to the FGF hypothesis, all three processes are regulated by a gradient of FGF.[1] We were interested in lens development as a model for studying cholinergic mechanisms in the embryo. During formation and invagination of the lens placode and later on during migration through the equatorial zone and elongation to lens fibers, the cells of the lens possess cholinesterase activity.[2,3] Expression of cholinesterase activity during phases of morphogenesis is a general phenomenon in embryonic tissues. To elucidate the role of cholinesterases (ChE) during embryonic development, one line of research followed the assumption of a primitive muscarinic system involved in morphogenesis,[4] whereas the other was accumulating evidence for noncholinergic functions of the cholinesterase proteins.[5] In the equatorial zone of the lens, phases of proliferation and differentiation are not only separated on the time axis, but also spatially by a zone of cell migration. Because of the specific spatial arrangement, the embryonic lens is a good model to study the interrelationship of these processes and to test whether the embryonic cholinergic system is involved in cell movement.

In the current study, we showed by histochemistry and immunohistochemistry that in the lens the phases of morphogenesis and differentiation are accompanied by cholinesterase activity, together with expression of the muscarinic cholinergic receptors (mAChR) and choline acetyltransferase (ChAT). To test the biological function of the muscarinic cholinergic system, embryonic lenses were isolated, loaded with fura-2/AM, and studied under an inverted fluorescence microscope. After stimulation with carbachol intracellular calcium mobilization and cell movement was monitored. Effects on cell movement were assessed by size measurements in single frames of a digital time-lapse video. Concomitant with the muscarinic Ca^{2+} mobilization, we observed a contraction of the whole embryonic lens.

The adult eye is a classic target for muscarinic cholinergic drugs. The nonneuronal cholinergic system of the eye has been reviewed by Duncan and Collison.[6] During treatment of glaucoma with cholinesterase inhibitors, cataract was observed as a side effect. Muscarinic effects were studied in isolated adult human lenses. Using fura-2/AM in whole lenses, it was shown that calcium mobilization could be induced in the anterior epithelium by muscarinic stimulation but not in the equatorial zone.[7] Reversible membrane depolarization in whole lenses and Ca^{2+} mobilization in cultivated anterior lens epithelial cells were induced after stimulation with acetylcholine.[8,9] The muscarinic antagonist atropine was shown to inhibit the excessive characteristic of chick form-deprivation myopia.[10] These are cholinergic effects on the postnatal morphogenesis of the optic cup and sclera. In the early chick embryo mAChR is expressed in general in migrating cells and blastemas during phases of morphogenesis.[4] In the present experiments this general phenomenon was studied in the embryonic lens.

Methods

Isolation and Dye Loading of Embryonic Lenses

Fertilized eggs of White Leghorn chickens (*Gallus gallus domesticus*) were obtained from a hatchery and incubated at 37.5°C in a temperature-controlled brooder. Lenses were removed from embryos at day 4 (Hamburger-Hamilton [HH] stage 21) with tungsten needles and fine forceps. The lens was carefully separated from the vitreous body with fine forceps. The isolated lens was placed in Hanks-HEPES solution containing 2 μmol/L fura-2 (MoBiTec; Molecular Probes, Göttingen, Germany). Loading took place at room temperature for 30 minutes. After loading, each lens was rinsed in 1 mL DMEM (Invitrogen-Gibco, Karlsruhe, Germany) that had been conditioned under an atmosphere of 5% CO_2 at 37°C. The lens was surrounded by a transparent, sticky

From the [1]Institute of Anatomy, Department of Experimental Embryology, and the [2]Institute of Anatomy, Department of Cellular Neurobiology, University of Tübingen, Tübingen, Germany.

Submitted for publication March 13, 2003; revised July 18, 2003; accepted July 30, 2003.

Disclosure: **M. Oppitz**, None; **A. Mack**, None; **U. Drews**, None

The publication costs of this article were defrayed in part by page charge payment. This article must therefore be marked "*advertisement*" in accordance with 18 U.S.C. §1734 solely to indicate this fact.

Corresponding author: Ulrich Drews, Anatomisches Institut, Österbergstr. 3, D-72074 Tübingen, Germany; udrews@anatom.uni-tuebingen.de.

halo of incipient vitreous body substance and single mesenchymal cells, which were removed with forceps. Anchoring was obtained by gentle pressure with microinstruments (tungsten needle or microforceps).

Measurement of Intracellular Ca^{2+}

Isolated lenses were immersed in a 400-μL drop of DMEM on a polylysine-coated glass coverslip that had been marked with a wax-based marker pen (Dako, Hamburg, Germany) to avoid overflow of droplet. The coverslip was placed in a cutout plastic Petri dish, fixed with silicone, and kept under constant gassing with an atmosphere of 5% CO_2/air during measurement.

Fura-2 fluorescence was monitored by the one-wavelength method at 380-nm excitation and 500-nm emission wavelengths. The one-wavelength method allowed the use of a digital charge-coupled device (CCD) camera (Fview; Soft Imaging Systems, Leinfelden-Echterdingen, Germany) without residual light amplification but with high resolution for time-lapse video microscopy. Comparative measurements showed coincidence between both methods.[11]

Application of Reagents

Acetylcholine, carbachol, ionomycin, and atropine were obtained from Sigma-Aldrich (Taufkirchen, Germany). Reagents were diluted in 0.1 M Hanks-HEPES solution (Invitrogen-Gibco). Single pulses of acetylcholine, carbachol, atropine, or ionomycin were applied under the microscope manually by an adjustable, photometrically calibrated micropipette made from borosilicate glass capillaries of 1.0 mm external diameter (World Precision Instruments, Sarasota, FL). Single pulses were applied without stirring the sample.

Time-Lapse Microscopy

Time-lapse studies on isolated lenses were performed with a microscope (model AX 50; Olympus, Hamburg, Germany) equipped with a temperature-controlled observation chamber (Solent Scientific, Inc., Portsmouth, UK) and a sensitive, computer-controlled, digital cooled chip CCD camera (Fview; Soft Imaging Systems). Images were taken at regular intervals (2 to 4 seconds, depending on required exposure time of camera) with computer-based time-lapse control. image processing software (AnalySIS, ver. 3.0; Soft Imaging Systems) was used to determine changes of mean pixel gray value (16-bit frame) within a limited section of each image in a series. Changes in intracellular calcium were assessed by its emission curve. The morphometry tool included in the software was used for interactive measurements of area from the series of images that had either been taken by fluorescence and by phase-contrast optics, respectively.

Histochemistry and Immunostaining

Isolated chick embryos were fixed in 4% buffered *para*-formaldehyde for 2 hours. Then, samples were rinsed and kept at 4°C in 30% sucrose for 24 hours. Samples were frozen at −70°C in optimal cutting temperature compound (Tissue-Tek; Miles, Elkhart, IN), and cut into 7-μm-thick sections. Cryostat sections were mounted on 3-amino-propylsylane (APS)–coated (ICN Biomedicals, Inc., Aurora, OH) slides and left to dry at 37°C overnight. Tissues underwent a preincubation step with 1% normal rabbit serum (Dako). Cryostat sections were incubated either with the M35 mAb (1:500; Argene Biosoft, Varilhes, France) or with an anti-ChAT mAb (1:10; Roche Diagnostics, Mannheim, Germany) at 4°C overnight, followed by 60 minutes incubation with 1:250 Cy3-conjugated rabbit anti-mouse IgM (Linaris, Wertheim, Germany). Nucleic acids were counterstained with Sytox green (1:50,000; Molecular Probes) for 5 minutes. After embedding in protective fluorescence mounting medium (Vector Laboratories, Burlingame, CA), samples were either examined with an epifluorescence microscope and digital cooled-chip camera or with a confocal laser scanning microscope with He-Ne laser and appropriate filter sets (LSM 410; Carl Zeiss Meditec, Oberkochen, Germany).

For staining with the M3 subtype specific anti-mAChR antibody, chick embryos were fixed in 4% buffered *para*-formaldehyde, dehydrated, and embedded in paraffin. They were cut into sections of 5-μm thickness, and mounted on APS-coated slides. After deparaffinization and rehydration, tissues were incubated with anti-M3 polyclonal antibody (1:1000; Biotrend, Cologne, Germany) at 4°C overnight, followed by a 90-minute incubation with biotin-conjugated rabbit anti-mouse IgG (1:500; Dako) and 90 minutes with peroxidase-coupled streptavidin (1:200; Dako). Staining was accomplished with 3-amino-9-ethylcarbazole (AEC) substrate (Vector Laboratories) for 20 minutes. Nucleic counterstaining was performed with 0.1% Mayer's hemalum for 5 minutes.

ChE activity was demonstrated histochemically with the procedure of Karnovsky and Roots.[12] The enzymatic reaction was performed in tissues after formalin fixation, embedding in water-soluble polyethylene glycol using established procedures.[2]

Results

Colocalization of Cholinesterase Activity and Muscarinic Receptors

During lens development in the chick embryo histochemical cholinesterase (ChE) activity first appeared in the lens placode. After invagination and formation of the lens, ChE activity concentrated in the elongating lens fibers in the posterior lens epithelium. In the HH stage-21 lens (Fig. 1A) single cells in the anterior epithelium and the equatorial zone showed a faint staining, and a prominent reaction in the elongating primary lens fibers, with enhanced deposition of reaction product in the apical cell poles.

In the section shown, the retina with differentiating positive ganglion cells and the surface ectoderm with single positive cells is closely apposed to the lens, because of dehydration during embedding in polyethylene glycol. Tests with specific blockers and substrates to distinguish between unspecific butyryl-cholinesterase (BChE) and specific acetylcholinesterase (AChE) showed that in the chick embryo lens the ChE activity corresponds to AChE.[2] In contrast, in the rat embryo lens in the same stage of development BChE was present in the same localization (results not shown). Layer et al.,[5] working with the chick embryo, noted a preponderance of BChE during proliferation and of AChE during differentiation. They also observed AChE in the elongating lens fibers of the chick embryo lens.

To clarify whether the ChE activity in the lens colocalizes with the mAChRs we performed an immunohistochemical study. Figure 1B shows an oblique paraffin-embedded section of the chick embryo lens in a slightly advanced stage of development, stained with the subtype M3-specific polyclonal antibody against mAChR used by Ndoye et al.[13] In the equatorial zone single strongly reacting cells appeared at the beginning of elongation (Figs. 1B, 1D). The cells resembled the ChE-positive droplet or flask cells observed in the primitive streak of the chick embryo at the epithelial–mesenchymal transition.[2] A homogeneous mAChR reaction was observed in all elongating lens fibers in the posterior lens epithelium. Faint nuclear counterstaining revealed the structure of the anterior lens epithelium (Fig. 1B) covered by the surface ectoderm that reacted positively for mAChR.

Comparison of mAChR and Anti-ChAT Immunoreactivity

Figure 2 depicts laser scanning microscopic images of sagittal cryostat sections from the equatorial zone of the lens anlage of a stage-21 chick embryo. Immunohistochemistry of the mAChR, using the mAb M35, was compared with anti-ChAT immunoreactivity. The mAb M35 is directed against the ligand-binding site of mAChRs and has no subtype specificity.[14,15] mAChR was localized in the elongating epithelial cells of the equatorial zone (Fig. 2A). A strong reaction of single cells, as in the paraffin-embedded sections was also identified, although

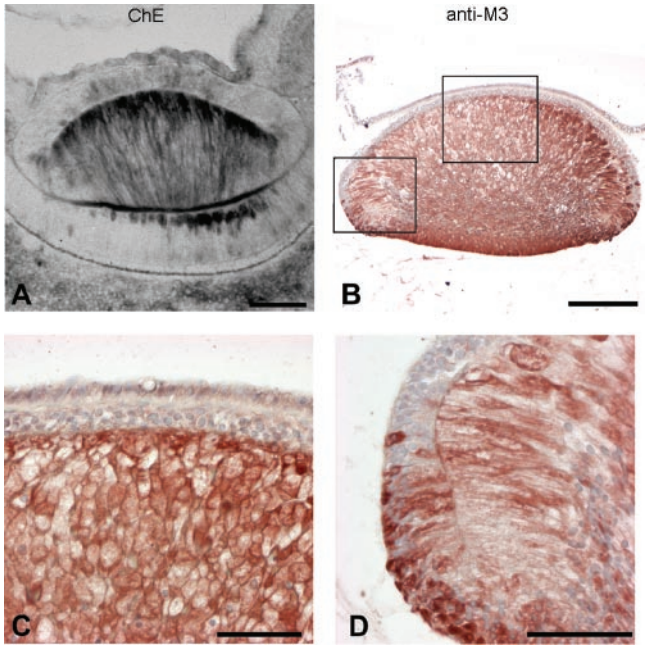

FIGURE 1. ChE activity and mAChR colocalized in the embryonic chick lens (HH stage 21). (**A**) Histochemical ChE activity was present in elongating primary lens fibers and in single cells of the equatorial zone and anterior lens epithelium. There was high activity in developing retinal neurons and moderate activity in the surface ectoderm. ChE reaction according to Karnovsky and Roots[12]in sections embedded in polyethylene glycol. (**B**) Subtype M3-specific immunoreactivity in a paraffin-embedded section was present in the equatorial zone and elongating lens fibers. Plane of section is oblique. (**C**, **D**) Higher magnifications of areas within *boxes* in (**B**). Reactivity was low in the anterior lens epithelium. (**C**) There was moderate reactivity in the surface ectoderm. (**D**) High immunoreactivity was visible in single cells in the equatorial zone. Bar: (**A**, **B**) 100 μm; (**C**, **D**) 50 μm.

not with the same clarity (compare Figs. 1D and 2A). In the lens fibers of the posterior epithelium, immunoreactivity was concentrated in the basal poles of the cells. The location of single cells in the row of elongating fibers was visualized by nuclear staining with Sytox green (Molecular Probes) in the same section (Fig. 2C). The reaction disappeared after the primary antibody had been omitted (Fig. 2B).

In a parallel cryostat section, immunoreactivity was visualized with a human anti-ChAT polyclonal antibody (Fig. 2D). Immunoreactivity was localized in the lens fibers of the posterior epithelium, whereas the cells in the anterior epithelium and in the equatorial zone were negative. In addition strong immunoreactivity was observed in the surface ectoderm and in mesenchyme at the entrance to the optic cup.

In conclusion, mAChR localized in the center of the equatorial zone between the zone of proliferation and differentiation, where cell migration occurs. The maximum expression of mAChR was observed in single cells during transformation of the anterior lens epithelium and subsequent elongation to primary lens fibers. The source of acetylcholine seemed to be the posterior pole of the lens.

Ca^{2+} Mobilization

Lenses were isolated from chick embryos HH stage 19 to 21, loaded with fura-2/AM, and observed in a drop of medium (400 μL) by time-lapse video. Fura-2 fluorescence was monitored with the one-wavelength method at 380-nm excitation and 500-nm emission wavelengths. A significant fluorescence emission was observed only in the equatorial zone of the lens, and not in the lens center. The experimental protocol followed the scheme established for calcium measurements in cell suspensions.[11] After equilibration, lenses were stimulated by addition of 4 μL carbachol 4×10^{-1} M, resulting in a final concentration of 4×10^{-3} M, which corresponds to saturation at the receptor binding site. Figure 3A shows a lens at HH stage 21 before and after stimulation. Figure 3B demonstrates the time course of the reaction by plotting the gray-scale values in the time-lapse images in the area indicated in Figure 3A (see Video 1 in Appendix). Similar tracings were obtained when the area of measurement was moved within the fluorescent annular pad of the lens. Stimulation elicited a significant increase in intracellular Ca^{2+} (decline in fura-2 fluorescence emission) after approximately 20 seconds. The peak reaction was followed by a plateau phase, reaching a state of equilibration within 1 minute. Addition of atropine in a final concentration of 1×10^{-6} M resulted in a reversal from the plateau to the baseline. Addition of atropine before stimulation prevented the entire carbachol-induced reaction, thus indicating that mAChR were involved (results not shown). The experiment was terminated by addition of ionomycin. The decrease in fluorescence after permeabilization of the cellular membrane by ionomycin indicated the specificity and cellularity of the fluorescence. Nineteen positive measurements were performed with carbachol, two with acetylcholine, and four with atropine blockade. The peak reaction was always reproducible, whereas atropine-induced reversal of the plateau reaction was often indistinct.

Contraction of the Lens after Muscarinic Stimulation

During Ca^{2+} measurements we observed a contraction of the whole lens which occurred after muscarinic stimulation concomitant with the intracellular Ca^{2+} release. The observations

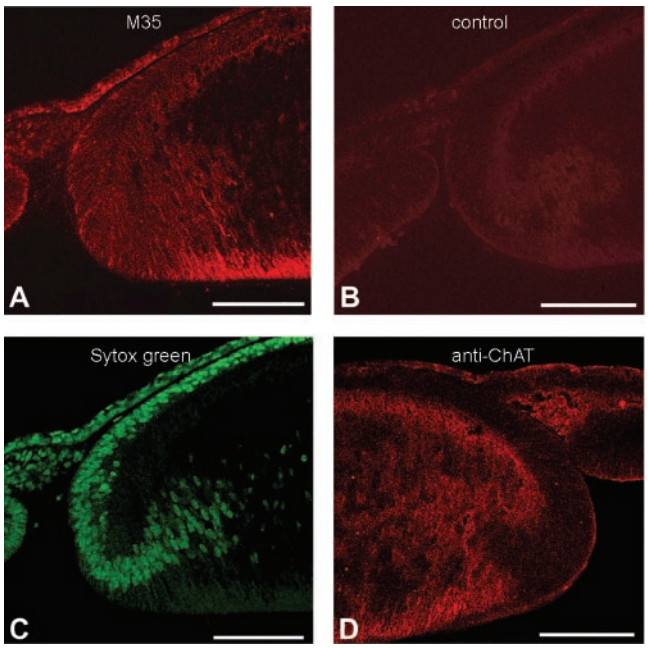

FIGURE 2. mAChR and ChAT immunoreactivity in cryostat-cut sections of embryonic chick lens (HH stage 21). Laser scanning microscope images: (**A**) Immunofluorescence with the M35 mAb. mAChR immunoreactivity concentrated in the basal parts of elongating lens fibers and in the equatorial zone. (**C**) Nuclear staining with Sytox green of the same section. (**D**) ChAT immunoreactivity in a parallel section. Prominent staining was present in elongating lens fibers and no staining in the equatorial zone. Distinct reactivity was visible in surface ectoderm and mesenchyme. (**B**) Control section processed without primary antibody. Bars, 100 μm.

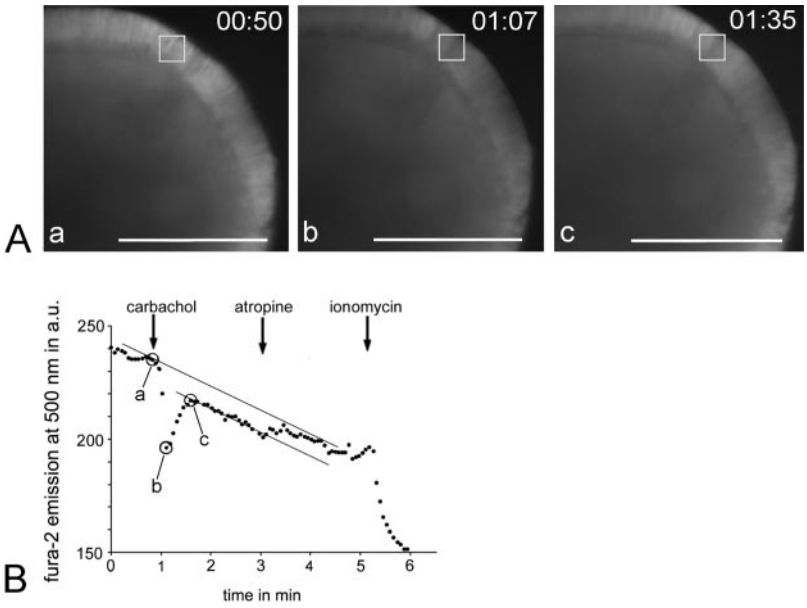

FIGURE 3. The isolated chick lens (HH stage 21) was loaded with fura-2/AM. Fluorescence was monitored under an inverted microscope and documented by a series of 90 images within 6 minutes (**A**). Fura-2 fluorescence is shown at the time points indicated in (**B**). Fluorescence was concentrated in the annular pad of the lens. The complete series of images is presented in a time-lapse video (See Appendix, Video 1). (**B**) The gray-scale value was quantitatively determined and depicted in arbitrary units. The window of measurement is indicated in (**A**). Due to leakage and fading, a declining baseline of fluorescence emission was recorded. After addition of carbachol, a decrease in fluorescence occurred (peak phase of Ca^{2+} mobilization), followed by a continuous lower level in fluorescence (plateau phase of extracellular Ca^{2+} influx). After addition of atropine, the fluorescence returned to the baseline (reversal of the plateau phase). Permeabilization of cell membranes by ionomycin indicated the cellularity of fluorescence. Bars, 100 μm.

were confirmed by three independent measurements of lens preparations, which had not been loaded with fura-2/AM and were stimulated under observation with phase-contrast optics (Figs. 4; see Video 2 in Appendix). In the time-lapse images the areas of the projected lens were measured by interactive circling using the built-in morphometry tool of the software (AnalySIS; Soft Imaging Systems). The changes in the circumference of the lens can be judged by comparison with the rectangle within the micrographs in Figure 4A. In the upper rim, the lens was more firmly fixed to the coverslip so that this area did not take part in the contraction movement. The tracing in Figure 4B shows that contraction of the lens started after a time lag of 20 seconds. Having reached its maximum after 120 seconds, the contraction was followed by a relaxation process that was accelerated by atropine. Within the observation time, the lenses did not entirely return to the original state.

Measurement of Lens Opacity

During the contraction of native lenses an increased light diffraction was observed under phase contrast optics which was clearly visible in the time-lapse video (Video 2). After addition of carbachol, the initially transparent central zone of the lens gradually darkened (Figs. 4A, 4C). The intensity of optical "darkness" was assessed by measuring the light intensity within a defined square in the center of the lens. In parallel with the lens contraction after the addition of carbachol to the bath, the lens opacity increased after approximately 20 seconds. Optical transparency reached a constant level at approximately 100 seconds after stimulation and increased slowly again when atropine was added. Without muscarinic stimulation, no change in opacity and no contraction occurred.

Coincidence of Ca^{2+} Release and Contraction

The time between stimulation and biological reaction varied because of the experimental setup and depended on the diffusion times of carbachol, added by micropipette. To determine the time course between transient Ca^{2+}-mobilization and contraction in the experiment depicted in Figure 5 (see Video 3 in Appendix), Ca^{2+} measurement and morphometry were performed in the same lens in the fluorescence images. Images were captured at an interval of 6.5 seconds. The peak reaction of Ca^{2+} and contraction started in the same frame. The Ca^{2+} peak ended after 32 seconds, whereas contraction reached its maximum after 1 minute. The Ca^{2+} tracing showed no effect on addition of atropine. The sudden change in size after addition of atropine has to be interpreted as an artifact due to optical changes. Permeation of the cell membranes by ionomycin caused a contraction wave that was regularly observed after addition of ionomycin at the end of the experiments.

DISCUSSION

Specificity of Immunostaining

In the early chick embryo, the muscarinic cholinergic receptors have been characterized in cell suspensions by binding and competition studies with [^{3}H] quinuclidinyl benzilate (QNB).[16] The competition studies with subtype-specific antagonists indicated the presence of the subtype M3. The mAb M35 is directed against the ligand-binding site and therefore has no subtype specificity.[15] The presence of mAChRs has been demonstrated by M35 immunohistochemistry and Western blot during ecdysone-induced morphogenesis of an epithelial cell line from *Chironomus tentans*[17] and by M35 immunohistochemistry in the isthmo-optic nucleus of the chick embryo.[18] Comparison of M35 immunohistochemistry and autoradiogra-

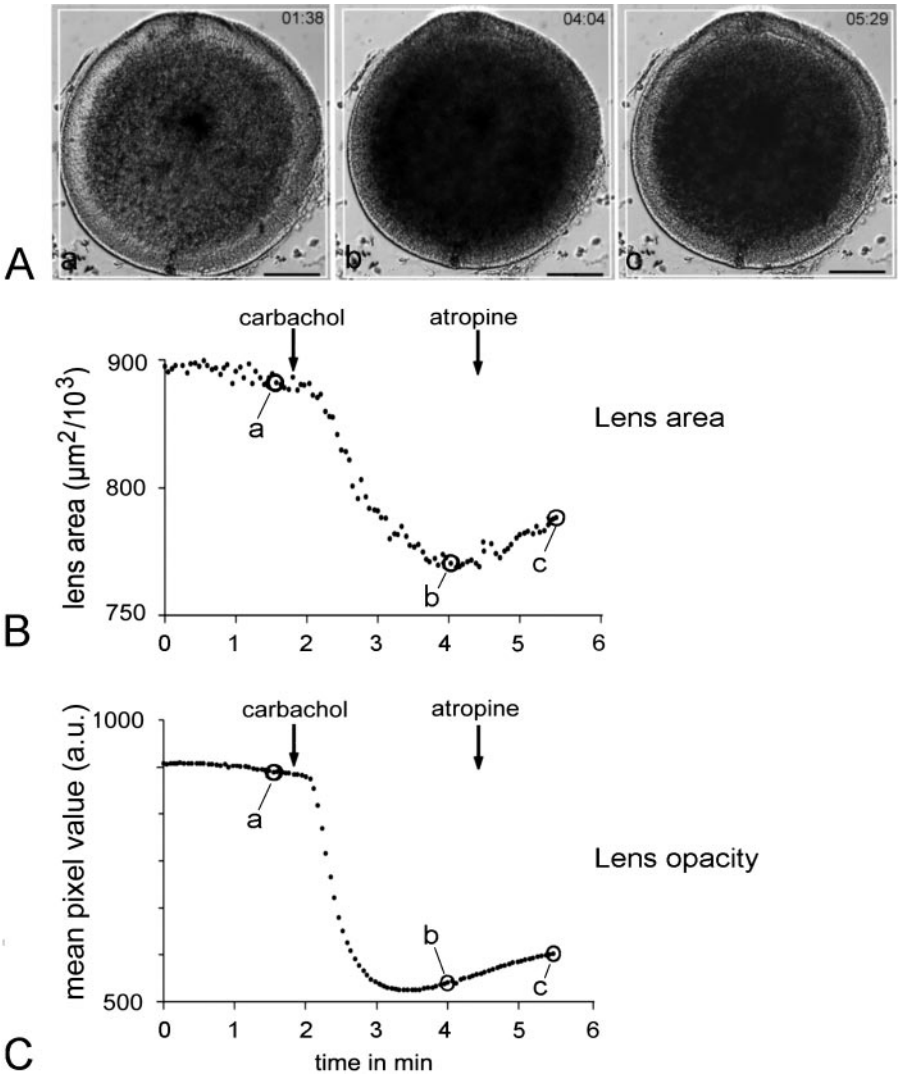

FIGURE 4. After isolation, the lens (HH stage 21) was directly transferred to the inverted microscope and monitored with phase-contrast optics. After addition of carbachol, the lens contracted and changed its opacity. Both effects were in part reversible by addition of atropine. (**A**) Images are shown before and after stimulation of carbachol and after addition of atropine. A *white rectangle* has been added to make the movement of the free rim more clearly visible. Bar, 100 μm. (**B**) Contraction was visualized by morphometry of the lens area. (**C**) The change in opacity was visualized by determining the mean pixel intensity in the center of the lens. The whole series of images is presented in a time-lapse video (see Appendix, Video 2).

phy with [^{3}H]QNB in mouse embryos revealed identical binding patterns.[19] Taking all these results together, we conclude that binding of M35 reliably identifies muscarinic receptor expression in embryonic tissues. The subtype-specific polyclonal antibodies of Ndoye et al.[13] are directed against the carboxyl termini of the receptor protein. The peptide used for immunization for the M3 subtype (SVHRTPSRCQ) shows the same alignment for the human and the chick cytoplasmic domain (calculation performed with BLAST; http://www.ncbi.nlm.nih.gov/ provided in the public domain by the National Center for Biotechnology Information, Bethesda, MD). The polyclonal antibody was used in paraffin-embedded sections and clearly labeled single cells in the equatorial zone, whereas, in the laser scanning microscope cryostat sections with M35, the predominant localization in cell membranes was visible.

Ca^{2+} Mobilization and Contraction

In the present study a carbachol-induced contraction was described. To demonstrate the biological relevance, the observation was correlated with measurements of muscarinic Ca^{2+} mobilization. The biphasic Ca^{2+} mobilization corresponded to the reaction in cell suspensions of embryonic cells[11] and in the human melanoma cell line SK-Mel-28 analyzed in earlier studies.[20] Stimulation of the embryonic mAChR resulted in an initial peak due to intracellular Ca^{2+} mobilization followed by a sustained plateau phase due to the influx of extracellular Ca^{2+}. The experiments demonstrating the receptor-gated extracellular influx during the plateau phase were performed in an earlier study.[11]

With a resolution of 6 seconds in the time axis the peak Ca^{2+} reaction occurred, and contraction started in the same video frame. The peak lasted approximately 30 seconds. Maximum contraction was reached after 1 minute. Addition of atropine reversed Ca^{2+} influx in the plateau phase and in some experiments led to a partial reversal of contraction and opacity (see Fig. 3/Video 1).

In earlier studies with embryonic tissues, the muscarinic cellular contractions have already been observed. In the chick blastoderm, perfusion with muscarinic agonists induced a contraction wave within 3 minutes.[21] Yamashita and Fukuda[22] described a contraction-like incurvation of the early embryonic retina after muscarinic stimulation. Perfusion of SK-Mel-28 melanoma cells with the muscarinic agonists acetylcholine and carbachol induced a retraction of cell membranes between focal adhesion points.[23] The present experiments correlated localization of mAChR with muscarinic agonist–induced Ca^{2+} mobilization and cellular contraction in the live embryonic lens. The increase in optical density of the living lens was presumably caused by a change of conformation of the actin

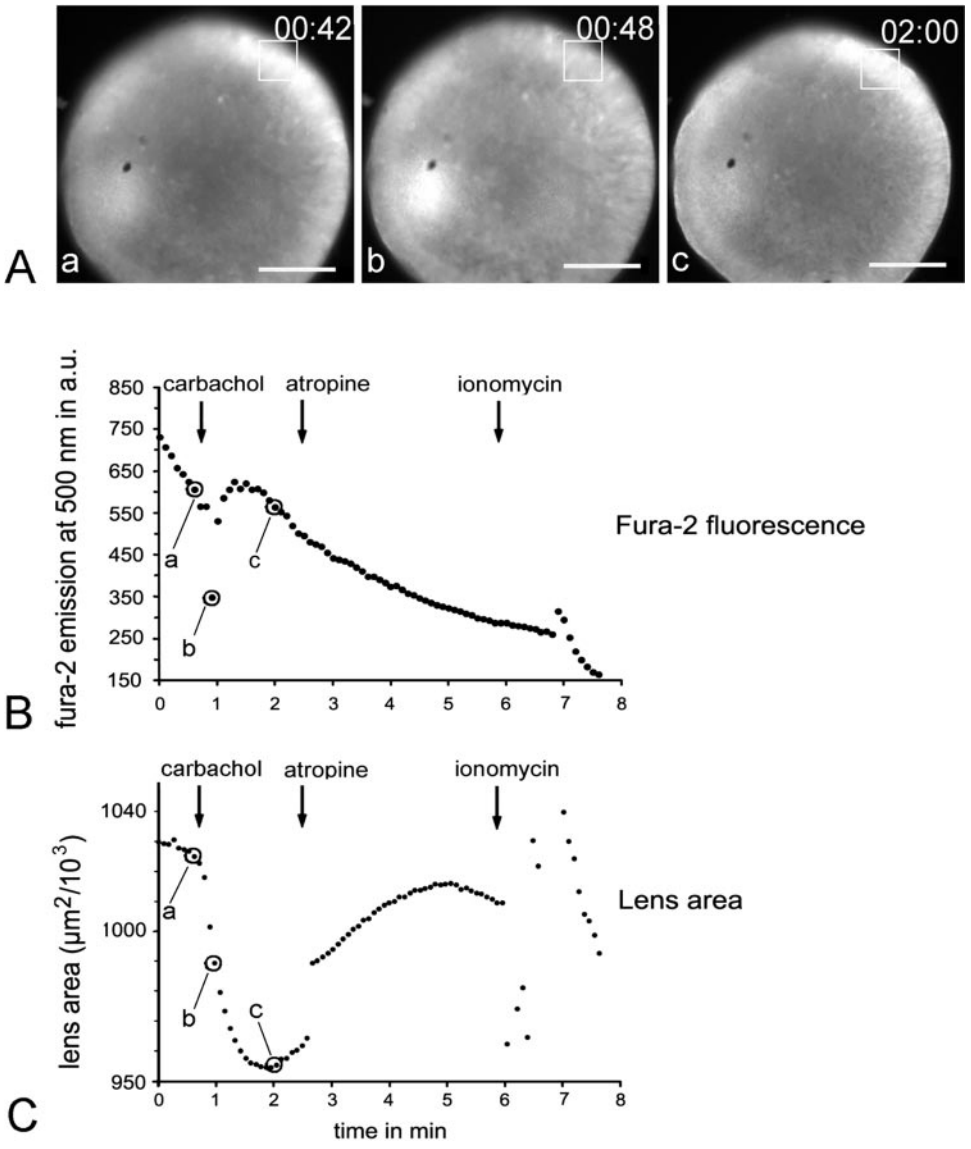

FIGURE 5. Coincidence of Ca^{2+} release and contraction after carbachol stimulation in a lens stage 21. (**A**) Single images of fura-2 fluorescence at the time points indicated in (**B**) and (**C**). (**B**) Tracing of fura-2 emission in the window indicated in (**A**). The peak of Ca^{2+} mobilization was visible approximately 10 seconds after stimulation and the contraction after approximately 10 seconds. A plateau phase was not visible. (**C**) Contraction measured as changes in area of lens projection. Atropine had only a small effect on the Ca^{2+} tracing, but resulted in a pronounced relaxation of contraction. The whole series of images is presented in a time-lapse video (see Appendix, Video 3). Bar, 100 μm.

cytoskeleton during contraction. F-actin has been found by others to be concentrated in the apical and basal ends of the epithelial cells and in elongating fiber cells.[24]

Muscarinic Receptors in the Adult Lens

Muscarinic agonists elicit a transient membrane potential in native human lenses[9] and Ca^{2+} release in cultured adult human lens cells.[8] The M1 subtype predominates in native human epithelial lens cells, whereas in the permanent lens cell line HLE-B3 and in primary cultures of lens cells the M3 subtype is mainly expressed.[8] The change in internal ion content observed in cataract lenses was associated with the muscarinic and purinergic Ca^{2+} release. In our experiments in the embryonic chick lens, we observed opacification as a reversible short-term effect in parallel to contraction.

In contrast, long-term effects of Ca^{2+} mobilization on proliferation and differentiation were described in adult lens cells.[6] In isolated lens cells, a biphasic reaction with a peak of intracellular mobilization and a plateau phase with extracellular influx were also observed in this context.[6] The dose–response curves and the agonist concentrations applied are in the same range as in the experiments described herein. In addition to the interpretation of the muscarinic effects in the embryonic lens under the aspect of morphogenesis, an interpretation as a developing functional trait observed in the adult lens is also feasible.

The Muscarinic System in the Morphogenesis of the Lens

Anti-ChAT immunoreactivity indicated that in the lens, acetylcholine synthesis occurs in the differentiating lens fibers. In an earlier study, acetylcholine synthesis in correlation to mAChR and ChE was demonstrated in the non-neural cells in the chick limb bud.[25]

Possible targets of the endogenous acetylcholine are the single cells with high mAChR immunoreactivity in the equatorial zone. Thus, the embryonic muscarinic system may function as a local regulator of morphogenesis, which occurs between proliferation and differentiation. Further experiments are needed to track morphogenesis in the lens down to single-cell movement.

Acknowledgments

The authors thank Leokadia Macher for providing excellent technical expertise and help with the experiments.

APPENDIX

Go to *http://www.iovs.org/cgi/content/full/44/11/4813/DC1* to view the following videos.

Video 1

Time-lapse video of fura-2 fluorescence in lens from an HH stage-21 chick embryo. Fluorescence emission was converted to pseudocolors for better visualization of changes. The 15-second video summarizes the observation period of 6 minutes, 6 seconds real time. At frame 01:07 minutes the decrease of fluorescence after addition of carbachol is visible (arrow). The time point of addition of carbachol, atropine, and ionomycin is represented by titles. The video is a higher magnification of the sample shown in Figure 3.

Video 2

A 17-second time-lapse video made from a series of phase-contrast images of a lens of an HH stage-21 chick embryo (real time 5 minutes, 29 seconds). At the upper margin, this lens was more firmly attached to the slide so that contraction was inhibited in this region. A white rectangle has been added to make the movement of the free rim more clearly visible. The time point of addition of carbachol, atropine, and ionomycin is indicated by titles. Changes in lens opacity and subsequent contraction of the lens vesicle start at time point 02:06 minutes, 20 seconds after addition of carbachol. This film corresponds to the diagrams in Figure 4. Bar, 100 μm.

Video 3

Video demonstrating the coincidence between Ca^{2+}-mobilization in the equatorial zone and the subsequent start of contraction of the lens. The three images shown in Figure 5 were taken from this video. Bar, 250 μm.

References

1. McAvoy JW, Chamberlain CG, de Iongh RU, Hales AM, Lovicu FJ. Peter Bishop Lecture: growth factors in lens development and cataract: key roles for fibroblast growth factor and TGF-beta. *Clin Exp Ophthalmol*. 2000;28:133–139.
2. Drews U. Cholinesterase in embryonic development. *Prog Histochem Cytochem*. 1975;7:1–52.
3. Layer PG, Sporns O. Spatiotemporal relationship of embryonic cholinesterases with cell proliferation in chicken brain and eye. *Proc Natl Acad Sci USA*. 1987;84:284–288.
4. Schmidt H. Muscarinic acetylcholine receptor in chick limb bud during morphogenesis. *Histochemistry*. 1981;71:89–98.
5. Layer PG, Keller M, Mack A, Willbold E, Robitzki A. Nonenzymatic roles of cholinesterases in avian neurogenesis: antisense BChE expression increases AChE expression, differentiation and apoptosis in retinal aggregates. In*: Structures and Functions of Cholinesterase and Related Proteins*. Bhupendra P, Taylor P, Quinn RL, eds. New York: Plenum Press; 1998:569–576.
6. Duncan G, Collison DJ. Role of the non-neuronal cholinergic system in the eye: a review. *Life Sci.* 2003;72:2013–2019.
7. Collison DJ, Duncan G. Regional differences in functional receptor distribution and calcium mobilization in the intact human lens. *Invest Ophthalmol Vis Sci*. 2001;42:2355–2363.
8. Collison DJ, Coleman RA, James RS, Carey J, Duncan G. Characterization of muscarinic receptors in human lens cells by pharmacologic and molecular techniques. *Invest Ophthalmol Vis Sci*. 2000;41:2633–2641.
9. Thomas GR, Williams MB, Sanderson J, Duncan G. The human lens possesses acetylcholine receptors that are functional throughout life. *Exp Eye Res*. 1997;64:849–852.
10. Stone RA, Lin T, Laties AM. Muscarinic antagonist effects on experimental chick myopia. *Exp Eye Res*. 1991;52:755–758.
11. Oettling G, Gotz U, Drews U. Characterization of the Ca^{2+} influx into embryonic cells after stimulation of the embryonic muscarinic receptor. *J Dev Physiol*. 1992;17:147–155.
12. Karnovsky HJ, Roots, WA. A "direct-coloring" thiocholine method for cholinesterase. *J Histochem Cytochem*. 1964;12:219–222.
13. Ndoye A, Buchli R, Greenberg B, et al. Identification and mapping of keratinocyte muscarinic acetylcholine receptor subtypes in human epidermis. *J Invest Dermatol*. 1998;111:410–416.
14. Andre C, Guillet JG, De Backer JP, Vanderheyden P, Hoebeke J, Strosberg AD. Monoclonal antibodies against the native or denatured forms of muscarinic acetylcholine receptors. *EMBO J*. 1984; 3:17–21.
15. Leiber D, Harbon S, Guillet JG, Andre C, Strosberg AD. Monoclonal antibodies to purified muscarinic receptor display agonist-like activity. *Proc Natl Acad Sci USA*. 1984;81:4331–4334.
16. Oettling G, Schmidt H, Drews U. The muscarinic receptor of chick embryo cells: correlation between ligand binding and calcium mobilization. *J Cell Biol*. 1985;100:1073–1081.
17. Lammerding-Koppel M, Spindler-Barth M, Drews U. 20-OH-Ecdysone-induced morphogenetic movements in a *Chironomus* cell line are accompanied by an expression of an embryonic muscarinic system. *Rouxs Arch Dev Biol*. 1994;203:439–444.
18. Calaza KC, Gardino, PF. Evidence of muscarinic acetylcholine receptors in the retinal centrifugal system of the chick. *Braz J Med Biol Res*. 2000;33:1075–1082.
19. Lammerding-Koppel M, Greiner-Schroder A, Drews U. Muscarinic receptors in the prenatal mouse embryo: comparison of M35-immunohistochemistry with [^{3}H]quinuclidinyl benzylate autoradiography. *Histochem Cell Biol*. 1995;103:301–310.
20. Noda S, Lammerding-Koppel M, Oettling G, Drews U. Characterization of muscarinic receptors in the human melanoma cell line SK-Mel-28 via calcium mobilization. *Cancer Lett*. 1998;133:107–114.
21. Drews U, Mengis W. Contraction wave in the chick blastoderm induced by muscarinic stimulation. *Anat Embryol* (*Berl*). 1990; 182:447–454.
22. Yamashita M, Fukuda, Y. Incurvation of early embryonic neural retina by acetylcholine through muscarinic receptors. *Neurosci Lett*. 1993;163:215–218.
23. Sailer M, Oppitz M, Drews U. Induction of cellular contractions in the human melanoma cell line SK-mel 28 after muscarinic cholinergic stimulation. *Anat Embryol* (*Berl*). 2000;201:27–37.
24. Beebe DC, Vasiliev O, Guo J, Shui YB, Bassnett S. Changes in adhesion complexes define stages in the differentiation of lens fiber cells. *Invest Ophthalmol Vis Sci*. 2001;42:727–734.
25. Reich A, Drews U. Choline acetyltransferase in the chick limb bud. *Histochemistry*. 1983;78:383–389.